ACS APPLIED MATERIALS & INTERFACES

RESEARCH ARTICLE

www.acsami.org

Role of Ion Flux on Alignment of Carbon Nanofibers Synthesized by DC Plasma on Transparent Insulating Substrates

Ryan C. Pearce,*[,†] Alexei V. Vasenkov,[‡] Dale K. Hensley,[§] Michael L. Simpson,[§] Timothy E. McKnight,[§] and Anatoli V. Melechko[†]

[†]Department of Materials Science and Engineering, North Carolina State University, Raleigh, North Carolina

[‡]CFDRC, Huntsville, Alabama

[§]Center for Nanophase Materials Science and [⊥]Measurement Sciences and Systems Engineering Division, Oak Ridge National Laboratory, Oak Ridge, Tennessee;

ABSTRACT: A key factor to the implementation of devices with vertically aligned carbon nanofibers (VACNFs) is fundamental understanding of how to control fluctuations in the growth direction of the fibers. Here we demonstrate synthesis of VACNF on transparent and insulating substrates by continuous direct current (DC) plasma for realization of cellular interface suitable for transmission optical microscopy. To maintain continuous glow discharge above the substrate, a metal grid electrode layer (Cr) was deposited over silica with windows of exposed silica ranging in size from 200μm to 1 mm. This electrode geometry allows for synthesis of VACNFs even within an insulating window. This observation and the observed trends in the alignment of nanofibers in the vicinity of grid electrodes have indicated that the alignment does not correspond to the direction of the electric field at the substrate level, contrary to previously proposed alignment mechanism. Computational modeling of the plasma with this grid cathode geometry has shown that nanofiber alignment trends follow calculated ion flux direction rather than electrical field. The new proposed alignment mechanism is that ion sputtering of the carbon film on a catalyst particle defines the growth direction of the nanofibers. With this development, fiber growth direction can be better manipulated through changes in ionic flux direction, opening the possibility for growth of nanofibers on substrates with unique geometries.

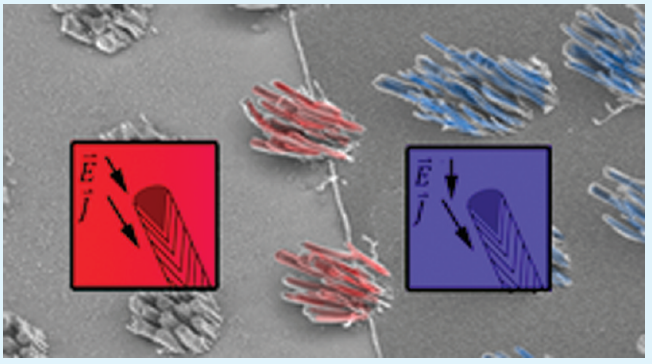

KEYWORDS: VACNF, carbon, nanofibers, PECVD, DC plasma, alignment

Vertically aligned carbon nanofibers (VACNFs) have a continually growing host of potential applications in devices with nanoscale functional elements such as gene and gene delivery arrays,[1] scanning probe tips,[2] electroanalytical probes,[2−4] electron field emission sources,[5−11] neural interfaces,[12−15] chemical and biosensors,[16,17] solar cells,[18−20] supercapacitors,[21,22] cell mimetic membranes,[23] and many others. Carbon nanofibers are made of stacked graphene "cups" or cones forming a cylindrical filamentous structure with diameters from a few nanometers to micrometers. Synthesis of CNFs is governed by processes which take place on a catalytic nanoparticle. Carbonaceous species decompose on a nanoparticle surface; carbon is then transported to a site where it is incorporated into a graphitic lattice. The location of the graphitic structure formed on the nanoparticle defines the direction of nanofiber growth.

In thermal chemical vapor deposition, the growth direction is random for an isolated nanofiber. Helveg et al have reported in situ observations of carbon nanofiber growth in which nanoparticle growth direction randomly changes depending on the graphitic carbon configuration formed after each lurching step.[24] There is no preference in growth direction defined by nanoparticle crystallographic orientation and the shape of the nanoparticle varies significantly during growth.[25]

Aligned growth has been observed in the presence of DC bias in plasma. Ren et al. showed that by performing the catalytic synthesis in DC plasma, the direction of nanofiber growth can be maintained perpendicular to the substrate.[26] Such vertically aligned carbon nanofibers can be grown in sparse arrays either from nickel catalyst dots that are defined lithographically[27] or from a thin catalyst layer. With electrically conductive substrates (such as Si), direct biasing has been used extensively. In response to observations that the direction of alignment correlates with electrical field lines, it has been suggested that the alignment mechanism involves the electrostatic forces on the nanofibers. One of the hypotheses stated that the electrostatic forces produce differential stresses on the nanoparticle/nanofiber interface that controls mass transport distribution and provides negative feedback to self-correct deviation from the direction

Received: June 3, 2011
Accepted: July 25, 2011
Published: July 25, 2011

of the electric field.[28] In a DC-PECVD chamber, the substrate acts as the cathode while the showerhead that introduces the process gases is the anode. Because of the need for an electric field to align the fibers, previously all substrates used for fiber growth in continuous DC plasma had to be conducting.

To sustain glow discharge at the catalyst location, we can simply connect the underlying electrically conductive substrate to the cathode. However, in fabrication of devices with VACNF elements, it is often necessary to provide isolation between the nanofibers or their groups. Several methods exist to grow VACNFs on insulating substrates, such as SiO_2. In one approach, the whole surface of a wafer is coated by a metal layer, which is removed after growth at the areas outside of the nanofibers and the connecting electrodes.[29] The use of pulsed DC plasma does not require continuous conduction path and allowed growth on metal micropads that are patterned prior to growth of VACNFs.[17,30−35] Alternatively, radio frequency sources can be used to sustain plasma with generated self-bias to provide vertical alignment.[36] The term vertical alignment means that the structures are perpendicular to the plane of the substrate.

Modification of the growth direction of carbon nanofibers in plasma synthesis has been achieved by varying geometry of the cathode and relative position of catalyst sites with respect to the electrode edges.[37] By varying electrode geometry the nanofiber growth has been directed to create structures with curved geometries.[38,39] Thus correlation between alignment of tip-type carbon nanofiber growth direction and the direction of the electric field in the vicinity of the substrate has been well established. However the exact coincidence of these directions, apart from a trivial case of growth on planar electrode far from the edge, has never been observed. Moreover, the calculated electrical fields were found to deviate from the measured nanofiber alignment directions.[37]

In this paper, we describe the alignment of carbon nanofibers on regions of transparent, fully insulating substrate as well as grid electrodes. The width of the insulating window within a metalized grid was varied to determine its effect on the morphology of VACNFs grown by continuous DC plasma. We hypothesize that ion flux direction, rather than electric field defines the growth direction. This hypothesis stems from (i) observation of vertically aligned tip-type CNFs at the center of insulating windows, (ii) observation of tilted CNFs on the metal electrodes, and (iii) strong pressure dependence of the nanofiber tilt.

METHODS

Substrate Preparation. Chromium strips were defined on two fused silica wafers with photolithography. First, P-20 primer was allowed to spread across the wafer for 10 seconds before being spun at 6000 rpm for 45 seconds to enhance the cohesion of photoresist. Negative tone NFR photoresist was then spun on the wafers at 6000 rpm for 45 s. The wafers were then baked at 115 °C for 90 s. A mask resulting in a wafer with the pattern shown schematically in Figure 1 was then exposed onto the wafers for 6 seconds at 9.45 mJ/cm^2 intensity on a contact aligner using a vacuum contact. The wafers were then given a post exposure bake at 115 °C for 90 s. Then, the two wafers were developed in CD-26 developer for 15 s before being rinsed with deionized water. Following development, the wafers were cleaned with oxygen plasma for 1 minute at 400W in a reactive ion etcher to remove excess photoresist before having 1000 Å of chromium deposited via electron beam evaporation. Liftoff was done in an acetone bath with assistance from an ultrasonic cleaner before being rinsed with IPA and dried. The wafers then had SPR 955 CM 0.7 photoresist spun on them at 3000 rpm for 45 s before being baked at 115°C for 90 s. A second mask was then used to create 2 μm diameter dots on the wafers. This mask was exposed with the same parameters as the first and followed an identical post-exposure procedure. Following the post-exposure procedure, the wafers had 500 Å of nickel deposited on them. Liftoff and cleaning was carried out as before. These steps resulted in two wafers with a grid of stripes underneath small nickel dots, which act as a catalyst for nanofiber growth

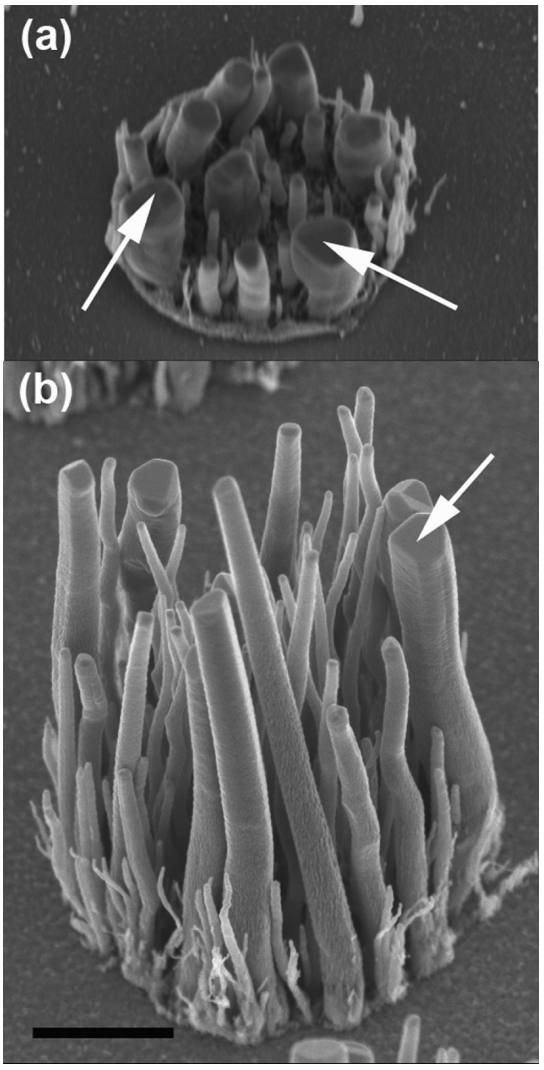

Figure 1. (a) SEM image of tip-type vertically aligned carbon nanofibers grown on fused silica in DC plasma. The arrows indicate the Ni catalyst nanoparticles. This VACNF cluster is ~200μm away from a grounded 100 nm thick chromium strip on the left and right. These fibers were grown at 15 Torr, 1A, and 550 V with 200 sccm NH_3 and 85 sccm C_2H_2. (b) SEM image of VACNFs on the same wafer as the one seen in a but grown on 100 nm thick chromium 400μm away on each side from fused silica. The scale bar represents 1μm for both a and b.

Nanofiber Synthesis. Fibers were then grown on the wafers in a custom built PECVD chamber. The parameters for growth were as follows: 700°C, 200sccms of NH_3, 85sccms of C_2H_2, 1 Amp with a ramp rate of 0.25 min, an etch on time of 10 s indicating that acetylene is allowed to run for 10 seconds before the plasma is sparked, and a growth time of 16 min. Processing

parameters have been explored to a great extent in literature. One wafer was run at 15 Torr, whereas the other was run at 4 Torr.

Imaging. Scanning electron microscopy of the fibers was done on a Zeiss Merlin FE-SEM at 5 kV. A nitrogen charge compensator was used for imaging of the insulating areas on the wafer. Optical microscopy was performed on a Nikon LV150 automated microscopy imaging system.

Simulation. We considered a 2D model of a dc glow discharge cell with a powered electrode being connected to the resistor-capacitor (RC) circuit. The system of equations of a dc glow discharge was solved using the CFD-ACE software,[40] and the RC circuit was modeled using SPICE software.[41] The plasma modeling and RC circuit simulations were coupled using an interface module. This module updates on- the-fly plasma current for the SPICE modeling and voltage at the powered electrode for the CFD-ACE simulations using CFD-ACE and SPICE output data, respectively. Chemical reactions and gas flow in a dc glow discharge are known to have a strong influence on gas temperature and neutral species spatial profiles in a Torr pressure range.[42] The effect of these processes on plasma density is not dominant and was neglected in the present simulations. This allows us to obtain a rapid steady state solution after approximately 10^5 time iterations. The time step in plasma simulations was controlled by the SPICE module and varied from 1×10^{-8} s to 1×10^{-9} s. The details of the model are given in refs 42 and 43.

Cell Culture and Imaging. U2OS, human osteosarcoma cells were cultured in DMEM/F12K supplemented with 10% fetal bovine serum and routinely passed at approximately 80% confluency. At passage, 1 mL of a suspension of U2OS ($\sim 10^6$ cells/mL) were plated upon a 100 mm VACNF wafer (as described) placed within a 125 mm dish containing 15 mL of supplemented media. Cells were imaged at 24 h intervals for a period of 4 days on a Nikon Diaphot 200 inverted phase contrast microscope at 200× magnification.

RESULTS AND DISCUSSION

Vertically aligned carbon nanofibers have been synthesized directly on regions of transparent, insulating substrate in a DC plasma. Figure 1 shows VACNF fibers that were grown by catalytic DC-PECVD on fused silica with a 100 nm thick chromium layer covering the wafer, except for "windows" of fused silica that were left uncovered. Fibers shown in Fig. 1a and 1b were grown at 15 Torr. The fibers in Figure 1a were grown on fused silica 100 μm from a chrome electrode on either side (i.e., in a "window"), whereas those in Figure 1b were grown directly on a chrome electrode. All of these VACNFs feature a catalyst nanoparticle (NP) at the tip, indicating a tip-type growth mode. In tip-type growth, a nanoparticle, which serves as the location for carbon deposition, is immersed in the anisotropic plasma environment where ion bombardment plays a significant role in governing surface decomposition, diffusion, and even particle temperature.[44,45] Base-type growth, where the NP remains at the substrate, has been observed to result in non-aligned nanofibers.[28] Such a scenario is likely to occur without an electrode grid on the substrate. Also, we expect that base-type growth may occur if the width of the bare fused silica windows were sufficiently large. Since the glow discharge cannot be maintained in a continuous DC plasma far away from grid electrodes, it becomes equivalent to thermal CVD conditions that produced base-type growth in this environment as has been reported elsewhere.[28] However in the range of window sizes from 0.2 to 1 mm, we only observed tip-type growth.

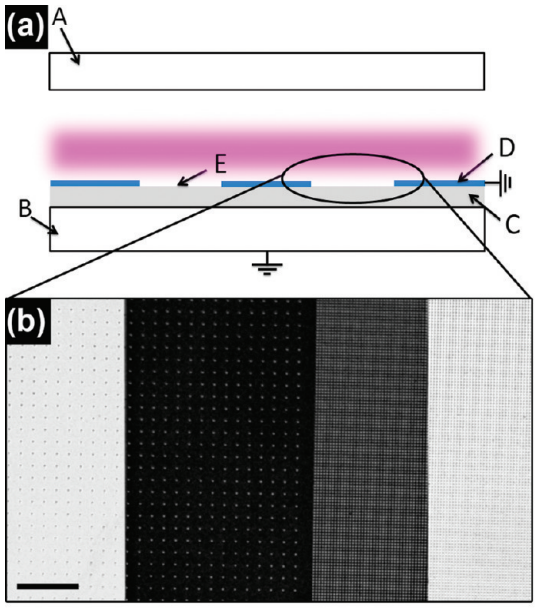

Figure 2. (a) Schematic of the reactor, electrode geometry, and wafer design: (A) anode that also acts as the showerhead where the process gases originate, (B) cathode that doubles as the substrate heater, (C) fused silica wafer, (D) 100 nm thick Cr "strips," (E) "windows" of fused silica left uncovered by Cr. (b) Optical micrograph of a fused silica window in between two Cr strips with the nickel catalyst dot pattern overlayed. The distance between Cr electrodes is 500μm. The scale bar corresponds to 100 μm.

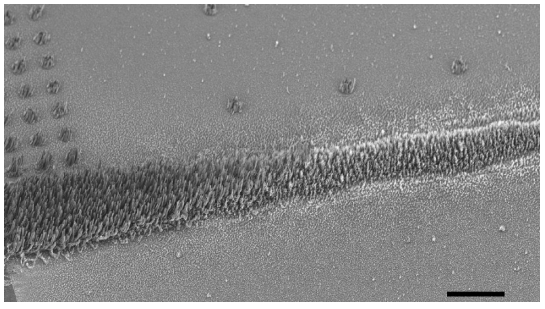

Figure 3. Transition across the Cr-fused silica interface can be seen clearly. The majority of the picture shows fused silica, whereas the interface can be seen in the bottom left corner of the image. The growth conditions cannot be optimal for such a strong difference in the substrate, explaining the difference in the character of the fibers. The scale bar represents 10μm.

A schematic of the reactor geometry is shown in Figure 2a. The window (E) width was varied from 0.2 mm to 1 mm across a 100 mm wafer in increments of 100μm to establish the correlation between nanofiber morphology and distance from a window. The glow was observed to cover the whole wafer including the fused silica windows. Figure 3 shows the variation of fiber growth as a function of distance from an electrode. The fibers on the interface have discernible tilt which straightens as the distance from the interface increases. The fibers also shorten further from the electrode. There is a significant, in case of Figure 1 an order of magnitude, difference in growth rate between nanofibers

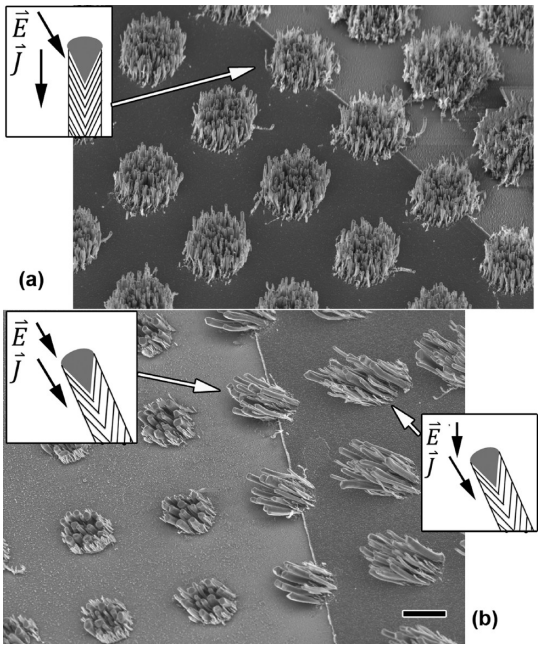

Figure 4. SEM images of the boundary between the electrode layer and insulating window. The images were taken at a 30° tilt. The fibers in Figure 3a were grown at 4 Torr while those in Figure 3b were grown at 15 Torr. At 4 Torr the fibers at the interface are nearly perpendicular with the substrate, whereas at 15 Torr, there is significant tilt. The insets indicate the approximate directions of the electric field (E) and ionic flux (J) determined from simulations. The electric field should remain nearly identical between the two, though the ionic flux will likely differ drastically as a function of pressure. At a pressure of 4 Torr the ionic flux must be perpendicular to the substrate, resulting in vertical fibers, whereas at 15 Torr the ionic flux is not perpendicular to the substrate, resulting in tilted fibers. This explanation is only true directly at the interface. Further into the electrode strip, the electric field will likely be more perpendicular to the substrate, though it is seen clearly in (b) that the fibers are tilted a few micrometers into the strip. The only cause for the fibers to remain tilted so far into the strip is that the ionic flux not being perpendicular. In each image, the distance between Cr electrodes is 600 μm. The scale bar corresponds to 1 μm.

grown on the electrode and the window. Such difference can be attributed to at least two factors: (i) the number of excited neutral radicals drops down away from electrode due to lowering of plasma density or (ii) the balance between etching and deposition of carbon on catalyst surface shifts away from optimum.[46]

The influence of electrical field on alignment of carbon nanofibers can be most prominently observed at the edge of the thin film electrode where it strongly varies. Figure 4 compares the fibers grown at 4 and 15 Torr at the boundary between the fused silica windows and the Cr electrode strips. At 4 Torr, the fibers on the interface between chrome and fused silica are perpendicular to the substrate, whereas the fibers on the 15 Torr sample are extremely tilted in the same area. The only parameter that was changed between the two is the pressure. With the bias remaining unchanged in this pressure range (4−15 Torr), the electric field direction does not change significantly within a few micrometers from the substrate. The increase in pressure leads to decrease in dark field size, where most of the voltage drop occurs, thus increasing the magnitude of the electric field. Because the alignment of nanofibers at these two pressures is drastically different, the electric field cannot be the alignment vector. Even at the base of the nanofibers indicated by an arrow in Figure 4b, located 3 μm from the edge of the electrode and only a few nanometers from the electrode surface, the tilt angle is significantly different from 90° with respect to the surface and it is the same as at the tip. A calculated direction of the electric field at such position over a flat metal surface is negligibly different from 90° with respect to the surface. This also serves as a strong indication that something else rather than electric field defines the growth direction.

Ion flux, on the other hand, can vary significantly depending on pressure. The estimated mean free path of ions changes from 14 to 4 μm when pressure changes from 4 to 15 Torr. Assuming that the balance between carbon deposition at the catalyst surface and its removal must be maintained in order for tip-type growth to occur,[28] the anisotropy vector of etch by ion bombardment can be such a defining direction. The direction of the ion flux is the factor that controls the removal of carbon film build up on a nanoparticle surface thus defining the nanoparticle motion. Others have measured the ion current density and found that below 15 ions/nm^2/s the carbon nanofibers follow the base-type growth regime, and that above 370 ions/nm^2/s the fibers were over-etched.[47] The insets in Figure 4 indicate the differences in the electric field and ionic flux, deduced from the nanofiber alignment, at the two pressures. The angle of the fibers is determined by the ionic flux vector in the vicinity of its catalyst particle as is demonstrated in Figure 4 where the vector is normal to the substrate at 4 Torr in the area near a chrome strip, but angled at 15 Torr in the same area. The electric field at the interface is likely to be nearly horizontal, but this edge effect would only occur within a fraction of a micrometer from the interface.[48]

Figure 5 shows the 2D profile of electrical potential a few micrometers above the surface calculated for 4 Torr total pressure (a), the profiles of electric potential and ion current density just above the wafer as a function of position in the x axis on the wafer (b), and the vector of ion current density a few micrometers above the surface (c). The potential has minimums and the ionic flux peaks at the chromium strips due to the ion acceleration in the sheath between the plasma and the grounded chromium strips. The ionic flux is non-zero in the fused silica areas because of the surface charge accumulation in these areas.

To explain variation of alignment and fiber height as a function of position with relation to the edge of the metal, we present the following model. Ion flux controls both the alignment and the growth rate of the fibers. The etch rate, which affects the growth rate, is determined by reactive etching and physical etching in the form of ion bombardment. The dependence of the alignment and growth rate can be explained by the directionality and rate of removal of carbon species on the catalyst particle. Carbon can interact with the catalyst nanoparticle in several ways. It can diffuse through the particle to form a graphene layer under the particle or it can adhere to the surface. The nanoparticle tip quickly becomes covered with a carbon layer during growth if there are few or no ions bombarding and volatilizing the deposited carbon. This carbon layer will halt growth, which is controlled by the amount of carbon which diffuses through the particle, unless it is removed. Therefore, there exists a maximum growth rate for a given process gas ratio and current, where etch regime does not outpace the carbon deposition and vice versa. Furthermore, the nanofiber will only grow in the direction from which the carbon is removed through a phenomenon called anisotropic etching. The ionic flux close to the edge of the chromium

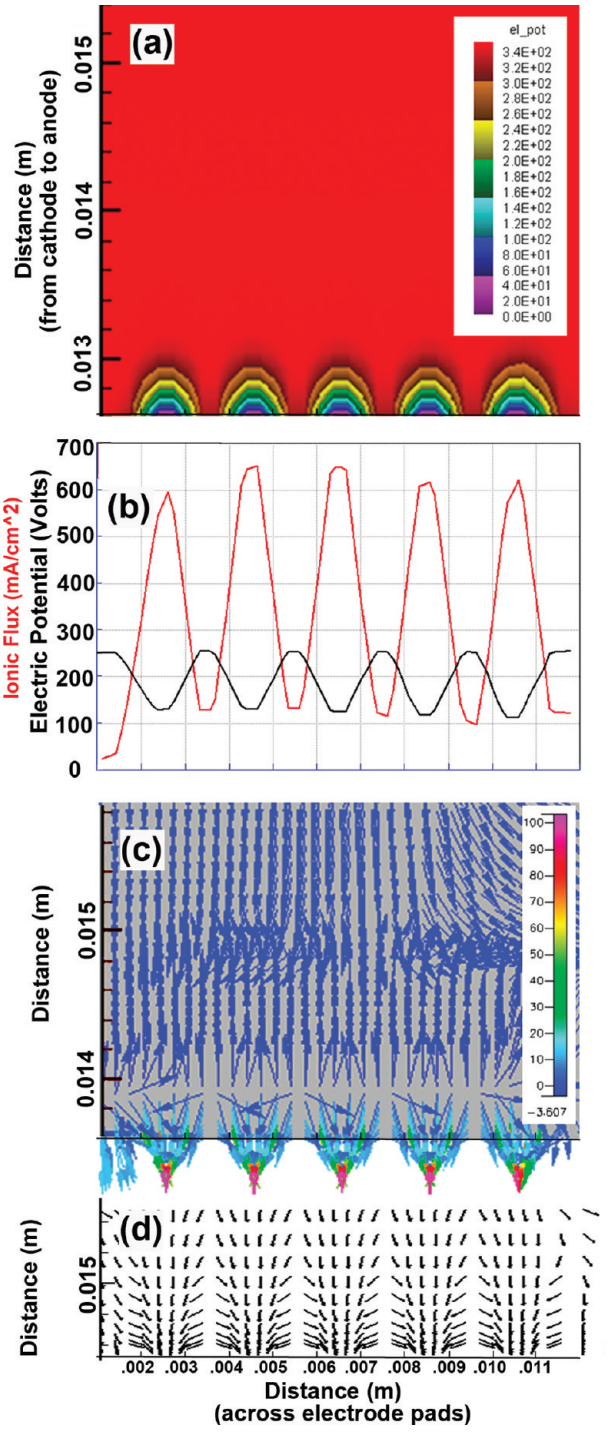

Figure 5. Graphs generated using the results of a CFD-ACE plasma modeling coupled with a SPICE circuit simulation at 4 Torr of total pressure. (a) 2D profile of electrical potential a few micrometers above the surface of the substrate. The electric potential reaches its minima at the grounded chromium strips, the conducting paths, while the minima for the ion flux are on the fused silica windows. (b) Profiles of electric potential and ion current density just above the wafer. (c) Vector of ion current density a few micrometers above the surface of the substrate. The ions are coulombically attracted to the grounded chromium strips which are in the locations of highest flux. The inertia of the ions, however, prevents them from precisely following the electric field lines and a fraction of them still bombard the surfaces that are nonconducting. (d) Electric field lines a few micrometers above the substrate surface.

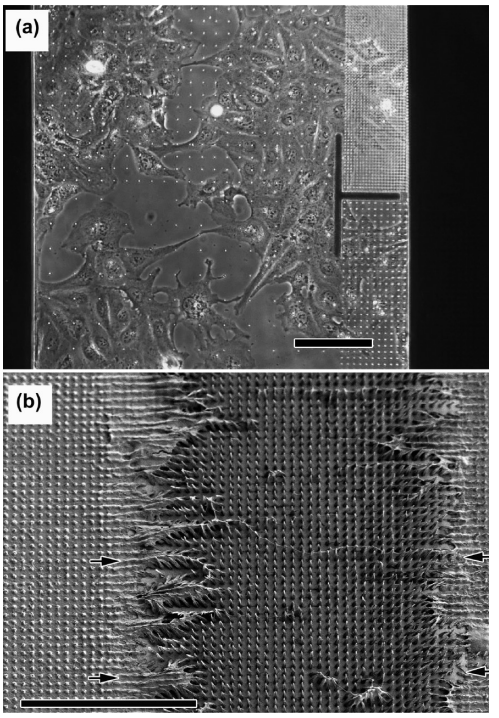

Figure 6. (a) Phase contrast optical micrograph and (b) scanning electron micrograph of human osteosarcoma cells (U2OS) cultured upon a VACNF array synthesized upon a transparent window on fused silica. The scale bar represents 100 μm. The arrows in (b) show the edge of Cr strip.

strips and fused silica is not perpendicular to the substrate, which leads to tilted fibers close to the interface, which become straighter the further they are from the interface. In reactive ion etching, ion bombardment is responsible for directional etching.[49] The anisotropy of distribution of chemical potential across the catalyst nanoparticle is believed to control the direction of catalyst motion.[50] Fiber height is controlled by etch rate, which is a function of current and pressure.[51]

Ultimately, the ability to grow VACNF on transparent substrates and control their geometry (alignment) at the nanoscale are essential to the application of VACNF arrays for cellular and tissue interfacing.[1,3,4,52,53] Transparent substrates enable the use of transmission (and specifically phase-contrast) microscopy thereby promoting visualization of the spatial relationship and dynamic interaction of the cellular matrix with VACNF elements.[54] Figure 6 a presents a phase contrast image of human osteosarcoma cells (U2OS) cultured upon the optically transparent window of a VACNF array grown as specified in this report, and provides clear visualization of subcellular organelles and individual VACNF elements. The ability to maintain nanofiber alignment normal to the substrate is necessary for efficient use of such arrays in impalefection, a gene delivery process in which nanofibers are pressed into cellular matrix or tissue.[55] Figure 6b shows variation of nanofiber alignment across an electrode strip in an SEM image of the same cell covered substrate as in Figure 6a. The nanofiber geometry is crucial in performing cellular impalement, i.e., it should be oriented with the direction of insertion. Thus nanofibers tilted with respect to the substrate would be undesirable. This study shows that growth at lower pressures (i.e., 4 Torr) is required to reduce the variation on the nanofiber deviation from the normal. This requirement puts limitation on the synthesis

process leading to significantly longer growth times necessary to achieve desired nanofiber length of a few tens of micrometers.[56] Engineering reactor/substrate geometries that provide ion flux uniformity at large pressure ranges are required for large-scale control of nanofiber alignment.

CONCLUSION

We have performed synthesis of vertically aligned carbon nanofibers in a DC plasma on an insulating substrate with a grid of electrodes. The alignment of the fibers has been observed to vary as a function of distance from the electrode grids. The pressures under which the fibers grow also play a large role in the tilt. It's been previously proposed that electrical fields on the surface of the substrate define the direction of the nanofiber growth. If that were the case the nanofibers at lower pressure (4 Torr) would be as tilted as nanofibers at high pressure (15 Torr), contrary to our observations. Theoretical calculations show that direction of ion flux diverges from the directions of electrical field vectors at the substrate level near the electrode edges. The trends in the calculated ion flux better fit the observed trends of nanofiber alignment. While observations provided here along with computational modeling support the hypothesis that ion flux controls the direction of nanofiber growth, it still remains to establish this correlation in direct experimental measurement of ion flux direction. These observations also help to choose the growth regime in implementation of nanofiber-based structures where function depends on the alignment (i.e., cellular impalement for gene delivery). A compromise between high growth rate (and large nanofibers) at high pressure and high normal alignment at low-pressure needs to be made depending on critical need for chosen functionality. With further understanding of how ionic flux determines morphology and alignment the possibility of a single reactor capable of synthesizing fibers with customized geometry is closer to reality.

AUTHOR INFORMATION

Corresponding Author
*E-mail: rpearce@ncsu.edu.

ACKNOWLEDGMENT

A.V.M. and M.L.S. acknowledge support from the Materials Sciences and Engineering Division, Office of Basic Energy Sciences, U.S. Department of Energy (processing, analytical microscopy, and experimental design). The device fabrication for cell interfacing was done through a user project at the Center for Nanophase Materials Sciences, Oak Ridge National Laboratory, and sponsored by the Scientific User Facilities Division, Office of Basic Energy Sciences, U.S. Department of Energy.

REFERENCES

(1) McKnight, T. E.; Melechko, A. V.; Hensley, D. K.; Mann, D. G. J.; Griffin, G. D.; Simpson, M. L. *Nano Lett.* **2004**, *4* (7), 1213–1219.
(2) Ye, Q.; Cassell, A.; Liu, H.; Chao, K.-J.; Han, J.; Meyyappan, M. *Nano Lett.* **2004**, *4* (7), 1301–1305.
(3) McKnight, T. E.; Mann, D. G. J.; McPherson, J. T.; Hoyt, P. R.; Melechko, A. V.; Simpson, M. L.; Sayler, G. S. *ACS Nano* **2008**, *2* (1), 69–76.
(4) McKnight, T. E.; Melechko, A. V.; Griffin, G. D.; Guillorn, M. A.; Merkulov, V. I.; Serna, F.; Hensley, D. K.; Doktycz, M. J.; Lowndes, D. H.; Simpson, M. L. *Nanotechnology* **2003**, *14* (5), 551–556.
(5) Chhowalla, M.; Ducati, C.; Rupesinghe, N. L.; Teo, K. B. K.; Amaratunga, G. A. J. *Appl. Phys. Lett.* **2001**, *79* (13), 2079–2081.
(6) Chhowalla, M.; Teo, K. B. K.; Ducati, C.; Rupesinghe, N. L.; Amaratunga, G. A. J.; Ferrari, A. C.; Roy, D.; Robertson, J.; Milne, W. I. *J. Appl. Phys.* **2001**, *90* (10), 5308–5317.
(7) Milne, W. I.; Teo, K. B. K.; Chhowalla, M.; Amaratunga, G. A. J.; Lee, S. B.; Hasko, D. G.; Ahmed, H.; Groening, O.; Legagneux, P.; Gangloff, L.; Schnell, J. P.; Pirio, G.; Pribat, D.; Castignolles, M.; Loiseau, A.; Semet, V.; Binh, V. T. *Diamond Relat. Mater.* **2003**, *12* (3-7), 422–428.
(8) Teo, K. B. K.; Chhowalla, M.; Amaratunga, G. A. J.; Milne, W. I.; Hasko, D. G.; Pirio, G.; Legagneux, P.; Wyczisk, F.; Pribat, D. *Appl. Phys. Lett.* **2001**, *79* (10), 1534–1536.
(9) Guillorn, M. A.; Yang, X.; Melechko, A. V.; Hensley, D. K.; Hale, M. D.; Merkulov, V. I.; Simpson, M. L.; Baylor, L. R.; Gardner, W. L.; Lowndes, D. H. *J. Vac. Sci. Technol., B* **2004**, *22* (1), 35–39.
(10) Choi, W. K.; Yun, J.; Wang, R.; Thong, J. T. L.; Thompson, C. V.; Zhu, M.; Foo, Y. L.; Hong, M. H. *Carbon* **2010**, *48* (5), 1362–1368.
(11) Guillorn, M. A.; Melechko, A. V.; Merkulov, V. I.; Hensley, D. K.; Simpson, M. L.; Lowndes, D. H. *Appl. Phys. Lett.* **2002**, *81* (19), 3660–3662.
(12) Li, J.; Nguyen-Vu, T. D. B.; Chen, H.; Cassell, A. M.; Andrews, R. J.; Meyyappan, M. *IEEE Trans. Biomed. Eng.* **2007**, *54* (6), 1121–1128.
(13) Li, J.; de Asis, E. D.; Nguyen-Vu, T. D. B.; Arumugam, P. U.; Chen, H.; Cassell, A. M.; Andrews, R. J.; Yang, C. Y. *Biomed. Microdevices* **2009**, *11* (4), 801–808.
(14) Cassell, A. M.; Li, J.; Nguyen-Vu, T. B.; Koehne, J. E.; Chen, H.; Andrews, R.; Meyyappan, M. *J. Nanosci. Nanotechnol.* **2009**, *9* (8), 5038–5046.
(15) Morrison, B.; Yu, Z.; McKnight, T. E.; Ericson, M. N.; Melechko, A. V.; Simpson, M. L. *Nano Lett.* **2007**, *7* (8), 2188–2195.
(16) Arumugam, P. U.; Yu, E.; Riviere, R.; Meyyappan, M. *Chem. Phys. Lett.* **2010**, *499* (4-6), 241–246.
(17) Li, J.; Ng, H. T.; Cassell, A.; Fan, W.; Chen, H.; Ye, Q.; Koehne, J.; Han, J.; Meyyappan, M. *Nano Lett.* **2003**, *3* (5), 597–602.
(18) Li, Z. Z.; Rochford, C.; Baca, F. J.; Liu, J. W.; Li, J.; Wu, J. *Nanoscale Res. Lett.* **2010**, *5* (9), 1480–1486.
(19) Rochford, C.; Li, Z. Z.; Baca, J.; Liu, J. W.; Li, J.; Wu, J. *Appl. Phys. Lett.* **2010**, *97*, 4.
(20) Na, J.-S.; Gong, B.; Scarel, G.; Parsons, G. N. *ACS Nano* **2009**, *3* (10), 3191–3199.
(21) Tse, K. Y.; Zhang, L. Z.; Baker, S. E.; Nichols, B. M.; West, R.; Hamers, R. J. *Chem. Mater.* **2007**, *19* (23), 5734–5741.
(22) Liu, J. W.; Essner, J.; Li, J. *Chem. Mater.* **2010**, *22* (17), 5022–5030.
(23) Fletcher, B. L.; Retterer, S. T.; McKnight, T. E.; Melechko, A. V.; Fowlkes, J. D.; Simpson, M. L.; Doktycz, M. J. *ACS Nano* **2008**, *2* (2), 247–254.
(24) Helveg, S.; Lopez-Cartes, C.; Sehested, J.; Hansen, P. L.; Clausen, B. S.; Rostrup-Nielsen, J. R.; Abild-Pedersen, F.; Norskov, J. K. *Nature* **2004**, *427* (6973), 426–429.
(25) Behr, M. J.; Mkhoyan, K. A.; Aydil, E. S. *ACS Nano* **2010**, *4* (9), 5087–5094.
(26) Ren, Z. F.; Huang, Z. P.; Xu, J. W.; Wang, J. H.; Bush, P.; Siegal, M. P.; Provencio, P. N. *Science* **1998**, *282* (5391), 1105–1107.
(27) Merkulov, V. I.; Lowndes, D. H.; Wei, Y. Y.; Eres, G.; Voelkl, E. *Appl. Phys. Lett.* **2000**, *76* (24), 3555–3557.
(28) Merkulov, V. I.; Melechko, A. V.; Guillorn, M. A.; Lowndes, D. H.; Simpson, M. L. *Appl. Phys. Lett.* **2001**, *79* (18), 2970–2972.
(29) Guillorn, M. A.; McKnight, T. E.; Melechko, A.; Merkulov, V. I.; Britt, P. F.; Austin, D. W.; Lowndes, D. H.; Simpson, M. L. *J. Appl. Phys.* **2002**, *91* (6), 3824–3828.
(30) Teo, K. B. K., *Rupesinghe* NL 7842135, 2010.
(31) Arumugam, P. U.; Chen, H.; Siddiqui, S.; Weinrich, J. A. P.; Jejelowo, A.; Li, J.; Meyyappan, M. *Biosens. Bioelectron.* **2009**, *24* (9), 2818−2824.
(32) Siddiqui, S.; Arumugam, P. U.; Chen, H.; Li, J.; Meyyappan, M. *ACS Nano* **2010**, *4* (2), 955−961.

(33) Koehne, J. E.; Chen, H.; Cassell, A. M.; Ye, Q.; Han, J.; Meyyappan, M.; Li, J. *Clin. Chem.* **2004**, *50* (10), 1886−1893.
(34) Cassell, A. M.; Li, J.; Stevens, R. M. D.; Koehne, J. E.; Delzeit, L.; Ng, H. T.; Ye, Q.; Han, J.; Meyyappan, M. *Appl. Phys. Lett.* **2004**, *85* (12), 2364–2366.
(35) de Asis, E.; Nguyen-Vu, T.; Arumugam, P.; Chen, H.; Cassell, A.; Andrews, R.; Yang, C.; Li, J. *Biomed. Microdevices* **2009**, *11* (4), 801−808.
(36) Caughman, J. B. O.; Baylor, L. R.; Guillorn, M. A.; Merkulov, V. I.; Lowndes, D. H.; Allard, L. F. *Appl. Phys. Lett.* **2003**, *83* (6), 1207−1209.
(37) Merkulov, V. I.; Melechko, A. V.; Guillorn, M. A.; Simpson, M. L.; Lowndes, D. H.; Whealton, J. H.; Raridon, R. J. *Appl. Phys. Lett.* **2002**, *80* (25), 4816–4818.
(38) AuBuchon, J. F.; Chen, L. H.; Gapin, A. I.; Jin, S. H. *Chem. Vap. Deposition* **2006**, *12* (6), 370–374.
(39) AuBuchon, J. F.; Chen, L. H.; Gapin, A. I.; Kim, D. W.; Daraio, C.; Jin, S. H. *Nano Lett.* **2004**, *4* (9), 1781–1784.
(40) Kolobov, V. I. *Comput. Mater. Sci.* **2003**, *28* (2), 302–320.
(41) Thorpe, T. W. *Computerized Circuit Analysis with SPICE : a Complete Guide to SPICE, with Applications*; Wiley: New York, 1992; p xix.
(42) Vasenkov, A. V. *J. Comput. Theor. Nanosci.* **2008**, *5* (1), 48–55.
(43) Vasenkov, A. V. Modeling Nanotube Synthesis: The Multiscale Approach. In *The Encyclopedia of Nanoscience and Nanotechnology*, 2nd ed.; Nalwa, H. S., Ed.; American Scientific: Stevenson Ranch, CA, 2011; Vol. V, 16, pp 281−302.
(44) Denysenko, I.; Ostrikov, K. *Appl. Phys. Lett.* **2007**, *90*, 25.
(45) Denysenko, I.; Ostrikov, K. *J. Phys. D: Appl. Phys.* **2009**, *42* (1), 12.
(46) Merkulov, V.; Melechko, A. V.; Guillorn, M. A.; Lowndes, D. H.; Simpson, M. L. *Chem. Phys. Lett.* **2002**, *361* (5-6), 492–498.
(47) Mauger, M.; Binh, V. T. *J. Vac. Sci. Technol., B* **2006**, *24* (2), 997−1003.
(48) Yoo, M. J.; Fulton, T. A.; Hess, H. F.; Willett, R. L.; Dunkleberger, L. N.; Chichester, R. J.; Pfeiffer, L. N.; West, K. W. *Science* **1997**, *276* (5312), 579–582.
(49) Coburn, J. W.; Winters, H. F. *Annu. Rev. Mater. Sci.* **1983**, *13*, 91–116.
(50) Merkulov, I. A.; Klein, K. L.; Simpson, M. L. *J. Appl. Phys.* **2009**, *105* (6), 064305.
(51) Merkulov, I. A.; Merkulov, V. I.; Melechko, A. V.; Klein, K. L.; Lowndes, D. H.; Simpson, M. L., *Phys. Rev. B: Condens. Matter Mater. Phys.* **2007**, *76* (1), 014109.
(52) Yu, Z.; McKnight, T. E.; Ericson, M. N.; Melechko, A. V.; Simpson, M. L.; Morrison, B. *J. Neurotraum.* **2007**, *24* (7), 1235–1235.
(53) McKnight, T. E.; Melechko, A. V.; Griffin, G. D.; Simpson, M. L. *In Vitro Cell. Dev. Biol.: Anim.* **2006**, *42*, 17a–17a.
(54) Hensley, D. K.; Melechko, A. V.; Ericson, M. N.; Simpson, M. L.; McKnight, T. E. Transparent microarrays of vertically aligned carbon nanofibers as a multimodal tissue interface. *Biomedical Sciences and Engineering Conference (BSEC) 2010*; Oak Ridge National Laboratory: Oak Ridge, TN, 2010; pp 1−4.
(55) Mann, D. G. J.; McKnight, T. E.; McPherson, J. T.; Hoyt, P. R.; Melechko, A. V.; Simpson, M. L.; Sayler, G. S. *ACS Nano* **2008**, *2* (1), 69−76.
(56) Melechko, A. V.; Klein, K. L.; Fowlkes, J. D.; Hensley, D. K.; Merkulov, I. A.; McKnight, T. E.; Rack, P. D.; Horton, J. A.; Simpson, M. L. *J. Appl. Phys.* **2007**, *102* (7), 074314-7.